PCCP

The Effect of Block Ratio on the Thermal Conductivity of Amorphous Polyethylene-Polypropylene (PE-PP) Diblock Copolymers

SCHOLARONE™
Manuscripts

The Effect of Block Ratio on the Thermal Conductivity of Amorphous Polyethylene-Polypropylene (PE-PP) Diblock Copolymers†

Xingfei Wei[*, a] and Tengfei Luo[a, b]

[a] Department of Aerospace and Mechanical Engineering, University of Notre Dame, Notre Dame, Indiana 46556, USA

[b] Center for Sustainable Energy at Notre Dame, University of Notre Dame, Notre Dame, Indiana 46556, US

* Corresponding author: Mr. Xingfei Wei. E-mail: xwei2@nd.edu. Tel: + 15749046870.

† Electronic supplementary information (ESI) available.

ABSTRACT

Block copolymers have a wide range of applications, such as battery electrolytes and nanoscale pattern generation. Thermal conductivity is a critical parameter in many of these applications (e.g., batteries), which is strongly related to the molecular conformation. In this work, the thermal transport in a representative diblock copolymer, polyethylene (PE)-polypropylene (PP), at different PE to PP block ratios are studied using molecular dynamics (MD) simulations. Our results show that the thermal conductivity of the PE-PP diblock copolymer can be tuned continuously by the block ratio, and it is strongly related to the molecular conformation, characterized by the radius of gyration (R_g). It is found that increasing the PP portion results in an overall decreasing trend in thermal conductivity since the PP block has a more flexible backbone, which leads to a smaller spatial extension of the whole PE-PP copolymer molecule. Thermal conductivity decompositions show that the bonding contribution is dominant in both the PE and PP portions of the block copolymer. The findings from this study can help understand thermal transport in general block copolymers.

1. Introduction

Block copolymers are widely studied in academic research and used in industrial applications, such as electrolytes in batteries[1-4] and nanoscale patterns for lithography.[5-12] For example, ion conductivity of the polymer is one of the most critical parameters for application in batteries. The copolymer chain conformation is found to be responsible for the increase in ion conductivity. A recent report shows that the ion conductivity of block copolymer membranes depends on the nanoscale morphology and the macroscopic connectivity conformation of copolymer chains.[2] Thermal conductivity of the polymer is an important parameter that is related to battery safety, which is also strongly related to chain conformation.[13-15]

The exploration of high thermal conductivity polymers has started a few decades ago. However, the thermal conductivities of amorphous polymers are mostly in the range of 0.1-0.5 W/mK.[27] Polymer chain alignment is one way of enhancing the thermal conductivity.[28-31] It is found that chain oriented polythiophene (PT) have a thermal conductivity as high as 4.4 W/mK, which is 20 times higher than that of the bulk PT.[18] Another method that can increase the polymer thermal conductivity is blending different polymers.[14, 32] In 2014, Kim et. al. reported that a poly(N-acryloyl piperidine) (PAP) and poly(acrylic acid) (PAA) amorphous blend thin film has a thermal conductivity as high as ~ 1.5 W/mK, due to the special chain conformation achieved from such blending.[32] Will block copolymers, which also display tunable microscopic conformations, enable high thermal conductivity?

Molecular dynamics (MD) simulation has been a powerful tool to study the thermal transport in polymers.[13, 33-35] A recent MD study shows that the hydroxyl groups (-OH) on alcohols can both

function as heat paths via coulombic interaction and create new heat paths via van der Waals (vdW) interaction.[36] Another recent MD study shows that increasing the side chain length on the bottlebrush polymers can decrease the thermal conductivity because energy scattering by the side chain increases.[15] Previously, our studies also show that the thermal conductivity of amorphous polymers is strongly related to the polymer conformation, such as the spatial extension of the polymer chains as characterized by radius of gyration (R_g) and persistence length (L_p).[13, 14] It is found that increasing the dihedral angle energy constant (chain stiffness) can increase R_g, which in turn increase the thermal conductivity.[13, 37] Meanwhile, increasing the inter-chain vdW interaction in polymer blends can also increase the R_g of the bulk polymer, which improves the thermal conductivity.[13, 14] For a diblock copolymer A-B, the molecule chain can be made of block A with a soft backbone and block B with a stiff backbone. The overall chain stiffness may be tuned by the block ratio, which may eventually change the copolymer conformation and thus thermal conductivity.

In this study, we use MD simulations to study the thermal conductivity of the most representative polyethylene (PE)-polypropylene (PP) diblock copolymers at different block ratios. The backbone of the PE block is comparatively stiffer than that of PP. By tuning the block ratio while keeping the total molecular length unchanged, the spatial extension of the block polymer is adjusted. The relationship between thermal conductivity and the block ratio is studied, which is further related to the polymer chain conformation (R_g). We have also decomposed the R_g and the heat flux into the PE and PP contributions to explore the mechanism of thermal transport in PP-PE diblock copolymers.

2. Simulation Model and Methods

All the MD simulations in this study are carried out using the Large-scale Atomic/Molecular Massively Parallel Simulator (LAMMPS). [38] Single chain PE-PP diblock copolymer models with 100 monomers on each chain are built by *Moltemplate*. [39, 40] Previous studies show that 50 monomers on each chain is sufficient to obtain converged thermal conductivity in the amorphous PE structure. [13, 14] The PP content in the PE-PP diblock copolymer is changed by replacing a portion of PE monomers with PP monomers (Fig. 1a-e). For example, when the PE-PP diblock copolymer has a PP content of 50%, it means 50 of the total 100 monomers are PP and the rest 50 monomers are PE. The Optimized Potential for Liquid Simulations of United Atom (OPLS-UA) is applied to simulate the interaction of the CH_3, CH_2, and CH groups in the system. [41] The OPLS-UA force field has been successfully used to model the thermal transport in amorphous PE systems, because the H atoms are at high vibrational frequencies (> 600 cm^{-1}) and have negligible contribution to thermal transport. [13, 14] The force field parameters are listed in the supplementary information (SI) section 1. [41] The thermal conductivity of the diblock copolymer is calculated as the following: The copolymer single chain is relaxed in the NPT ensemble (1 atm, 300 K), then it is duplicated to 400 molecules for simulating a bulk copolymer. The simulation box with 400 copolymer chains is relaxed in the NVT (600 K) and NPT (1 atm, 600 K) ensembles sequentially, until the molecule conformation (R_g) reaches the steady state. In SI section 2, we show an example of the copolymer structure relaxation process in the NPT ensemble (1 atm, 600 K). After the system is at equilibrium, the NVT ensemble (2 ns) is applied to further relax the structure at 600 K. Finally, the NVE ensemble is used with Langevin thermostats, which apply a temperature gradient across the simulation domain, to calculated the thermal conductivity by the non-equilibrium MD (NEMD) simulation method (Fig. 1).

The bulk block copolymer model has 400 chains in the cubic simulation box (length ~15 nm). Our results show that 400 chains are sufficient to eliminate the size effect of the calculated thermal conductivity of a bulk block copolymer (SI section 3, Fig. S4). The amorphous bulk copolymer structure is shown in Fig. 1f. The Langevin thermostat is applied to establish the heat source in the middle (orange box) and heat sink at the two ends (two blue boxes) (Fig. 1f). The energy input and output are recorded at both the heat source and the heat sink, which indicate that the system reaches the steady state (Fig. 1g). At the steady state, the slope of the energy input (or output) divided by the cross-sectional area yields the heat flux (J). The temperature profile of the copolymer structure at the steady state is shown in Fig. 1h. The temperature gradient (dT/dx) can be calculated by a linear fit of temperature profile (Fig. 1h, the red line). The thermal conductivity of the copolymer is calculated by the Fourier's law ($k = \frac{-J}{dT/dx}$).

In order to have a better understanding of the thermal transport mechanism inside block copolymers, the decomposition method is used.[13, 14, 42-44] The total heat flux can be attributed to the contributions from bonding and non-bonding interactions (Eq. 1).

$$J_{total} = J_{bonding} + J_{non-bonding} \tag{1}$$

The bonding interaction is the sum of the bond, angle and dihedral interactions (Eq. 2). The non-bonding interaction is the sum of the vdW and Coulombic interactions.

$$J_{bonding} = J_{bond} + J_{angle} + J_{dihedral} \tag{2}$$

Knowing the heat flux contributions from bonding and non-bonding interactions, the thermal conductivity can be decomposed as the following:

$$\kappa_{bonding} = \kappa_{total} * \frac{J_{bonding}}{J_{total}} \tag{3}$$

6

$$\kappa_{non-bonding} = \kappa_{total} * \frac{J_{non-bonding}}{J_{total}} \tag{4}$$

3. Results and Discussions

3.1 The Block Ratio Effect on Thermal Conductivity

The thermal conductivity of amorphous diblock PE-PP copolymer is found to depend on the PP block ratio. At 600 K, the pure PE has a thermal conductivity of ~ 0.14 W/m.K, and that of the pure PP is ~ 0.07 W/m.K (Fig. 2). When the PP block ratio increases the thermal conductivity decreases monotonically (Fig. 2). We note that the temperature is 600 K, since the amorphous structure of the copolymer can be more quickly equilibrated at high temperature. At room temperature (300 K), our model calculated thermal conductivity values of PE and PP are 0.24 and 0.12 W/m.K, respectively, which are similar to the published simulation and experimental data (PE 0.21-0.33 W/m.K, PP 0.1-0.22 W/m.K).[13, 27] Interestingly, when the PP content is below 10%, the PE-PP diblock copolymer has a thermal conductivity close to that of the pure PE. There appears to be a resistance in changing thermal conductivity when the PP block ratio increases initially (Fig. 2). A study shows that in graphyne heterojunctions the thermal conductivity decrease is related to the decrease in vibration density of states.[45] However, PE and PP have a similar chemical structure and the same backbone. We believe that the vibration density of states for PE-PP copolymers are similar at different PP block ratios. Previous studies show that in amorphous polymers the thermal conductivity is strongly related to the polymer chain conformation, such as R_g.[13, 14] In the following sections we will discuss how the block ratio can affect the block copolymer chain conformation and how this leads to the change in thermal conductivity.

3.2 The Conformation and Thermal Conductivity Relation in PE-PP Block Copolymers

The thermal conductivity and the polymer conformation can have a one-to-one relationship.[13,14,46] Figure 3a shows that the average molecular R_g of the PE-PP diblock copolymer decreases when the PP content increases. The relationship between the thermal conductivity and the R_g of the copolymer is plotted in Fig. 3b. It is generally conclusive that the thermal conductivity of amorphous block copolymers increases when the R_g increases (Fig. 3b). The reason is that the copolymer chain is more spatially extended when the R_g is large. The extended chain can make heat transfer more efficient, because the energy transfer along the chain is much more efficient than that between chains.[13, 14] In the next section we will discuss how the PE and PP portions can affect the conformation of the block copolymer chain and the corresponding thermal conductivity.

3.3 The Decomposition of R_g and Thermal Conductivity into PE and PP Contributions

The R_g of the PP portion and the PE portion are calculated separately for each PE-PP diblock copolymer molecule and then averaged over the 400 chains in the system (Fig. 4a). In general, as the PP content increases, the R_g of the PE portion decreases monotonically and that of the PP portion increases monotonically. At the PP content of 50%, the R_g of the PE portion is ~ 2.5 Å larger than that of the PP portion (Fig. 4a). This is because the backbone of the PP portion is softer than the PE portion, and thus with the same number of monomers the PE portion is more extended. For freely joined chains, R_g is known to be proportional to $\sqrt{N}$ (N is the number of monomers).[47] We use $\sqrt{N}$ to fit the R_g of PE and PP portions in the PE-PP diblock copolymer (Fig. 4a, blue-PE and red-PP lines), and both fit very well, which indicates that the PE and PP portions are very independent in conformation in the block copolymers.

For a block copolymer, the thermal energy transport can go through both the PE and PP portions. In the MD simulation, the heat flux can be decomposed into energy transport through the PE and PP portions (SI section 4).[13, 14, 33, 44, 48] Figure 4b shows the overall thermal conductivity and its decomposition into the PE and PP portions (PE-k and PP-k). The trends correlate very well with those observed in R_g. When the PP content increases, the thermal conductivity contributed by the PE portion decreases monotonically while that from the PP portion increases monotonically.

3.4 The Decomposition of Thermal Conductivity into Bonding and Non-Bonding Contributions

In polymers, the thermal energy can transport along the molecular chain by bonding interactions and between different molecules by non-bonding interactions. Figure 5a shows the thermal conductivity decomposition of bonding and non-bonding interactions for the PE-PP diblock copolymers. For the PE portion, the bonding contribution is dominant (Fig. 5a, solid green triangle), which decreases dramatically with the increase of the PP content. For the PP portion (Fig. 5a, brown diamond), the bonding contribution is similar to that from the non-bonding interactions, both of which change slowly with the increase of the PP content. The non-bonding contribution of the PP portion is larger than that of the PE portion when the PP content is at 50%. This is because the PP monomer has more particles than the PE monomer, and thus there are more pairs of atoms interacting with the non-bonding interactions. Even though non-bonding interaction (vdW) is stronger at high PP content, since its contribution to thermal conductivity is small, the total thermal conductivity is still not high.

Thermal transport along the polymer chain is strongly related to the molecular conformation (R_g). The relationship between the decomposed thermal conductivity and the R_g of the corresponding PE (or PP) portion is important to exploring the thermal transport mechanism (Fig. 5b). For the PE portion, the bonding contribution is strongly related to the R_g (Fig. 5b, blue line), when the R_g is higher than ~ 18 Å (Fig. 5b, black dash line). For the PP portion, the R_g is playing a less important role in the bonding contribution (Fig. 5b, red line). Figure 5b also shows that the non-bonding contribution is less important for both the PE and PP portion when the R_g increases, and that when the R_g is the same the non-bonding contribution from the PP portion is larger than that from the PE portion.

4. Conclusions

In this study, we use MD simulations to calculate the thermal conductivity of amorphous PE-PP diblock copolymers. Our results show that the thermal conductivity of the PE-PP diblock copolymer can be tuned by the PP block ratio. The thermal conductivity of block copolymers is found strongly related to the molecular conformation (R_g). The $\sqrt{N}$ fitting of the R_g for both the PE and PP portions shows that the PE and PP portions are very independent in conformation in the block copolymer. Thermal conductivity decomposition shows that the PE-k contribution decrease dramatically and the PP-k contribution increase slightly when the PP content increases. we also find that the bonding contribution is dominant in both the PE and PP portions. The non-bonding interaction is stronger at high PP content, but its contribution to thermal conductivity is small, therefore the total thermal conductivity at the high PP content is not high.

Competing Financial Interest

The authors declare no competing financial interest.

Acknowledgements

References

1 E. D. Gomez, A. Panday, E. H. Feng, V. Chen, G. M. Stone, A. M. Minor, C. Kisielowski, K. H. Downing, O. Borodin and G. D. Smith, Effect of Ion Distribution on Conductivity of Block Copolymer Electrolytes, *Nano Lett.,* 2009, **9**, 1212-1216.

2 R. L. Weber, Y. Ye, A. L. Schmitt, S. M. Banik, Y. A. Elabd and M. K. Mahanthappa, Effect of Nanoscale Morphology on the Conductivity of Polymerized Ionic Liquid Block Copolymers, *Macromolecules,* 2011, **44**, 5727-5735.

3 P. W. Majewski, M. Gopinadhan, W. Jang, J. L. Lutkenhaus and C. O. Osuji, Anisotropic Ionic Conductivity in Block Copolymer Membranes by Magnetic Field Alignment, *J. Am. Chem. Soc.,* 2010, **132**, 17516-17522.

4 S. Zhang, K. H. Lee, C. D. Frisbie and T. P. Lodge, Ionic Conductivity, Capacitance, and Viscoelastic Properties of Block Copolymer-Based Ion Gels, *Macromolecules,* 2011, **44**, 940-949.

5 L. Leibler, Theory of Microphase Separation in Block Copolymers, *Macromolecules,* 1980, **13**, 1602-1617.

6 F. S. Bates and G. H. Fredrickson, Block Copolymer Thermodynamics: Theory and Experiment, *Annu. Rev. Phys. Chem.,* 1990, **41**, 525-557.

7 H. Kim, S. Park and W. D. Hinsberg, Block Copolymer Based Nanostructures: Materials, Processes, and Applications to Electronics, *Chem. Rev.,* 2010, **110**, 146-177.

8 T. H. Epps III and R. K. O'Reilly, Block Copolymers: Controlling Nanostructure to Generate Functional Materials–synthesis, Characterization, and Engineering, *Chem. Sci.,* 2016, **7**, 1674-1689.

9 M. Matsen and F. S. Bates, Unifying Weak-and Strong-Segregation Block Copolymer Theories, *Macromolecules,* 1996, **29**, 1091-1098.

10 K. W. Guarini, C. T. Black and S. H. Yeung, Optimization of Diblock Copolymer Thin Film Self Assembly, *Adv Mater,* 2002, **14**, 1290-1294.

11 C. Tang, E. M. Lennon, G. H. Fredrickson, E. J. Kramer and C. J. Hawker, Evolution of Block Copolymer Lithography to Highly Ordered Square Arrays, *Science,* 2008, **322**, 429-432.

12 Y. Zhuang and P. Charbonneau, Recent Advances in the Theory and Simulation of Model Colloidal Microphase Formers, *J. Phys. Chem. B,* 2016, **120**, 7775-7782.

13 T. Zhang and T. Luo, Role of Chain Morphology and Stiffness in Thermal Conductivity of Amorphous Polymers, *J. Phys. Chem. B,* 2016, **120**, 803-812.

14 X. Wei, T. Zhang and T. Luo, Chain Conformation-Dependent Thermal Conductivity of Amorphous Polymer Blends: The Impact of Inter-and Intra-Chain Interactions, *Phys. Chem. Chem. Phys.,* 2016, **18**, 32146-32154.

15 H. Ma and Z. Tian, Effects of Polymer Topology and Morphology on Thermal Transport: A Molecular Dynamics Study of Bottlebrush Polymers, *Appl. Phys. Lett.,* 2017, **110**, 091903.

16 V. Sethuraman, V. Pryamitsyn and V. Ganesan, Influence of Molecular Weight and Degree of Segregation on Local Segmental Dynamics of Ordered Block Copolymers, *J. Polym. Sci. , Part B: Polym. Phys.,* 2016, **54**, 859-864.

17 H. Minehara, L. M. Pitet, S. Kim, R. H. Zha, E. Meijer and C. J. Hawker, Branched Block Copolymers for Tuning of Morphology and Feature Size in Thin Film Nanolithography, *Macromolecules,* 2016, **49**, 2318-2326.

18 V. Singh, T. L. Bougher, A. Weathers, Y. Cai, K. Bi, M. T. Pettes, S. A. McMenamin, W. Lv, D. P. Resler and T. R. Gattuso, High Thermal Conductivity of Chain-Oriented Amorphous Polythiophene, *Nat. Nanotechnol.,* 2014, **9**, 384-390.

19 L. D'orazio, R. Greco, C. Mancarella, E. Martuscelli, G. Ragosta and C. Silvesrte, Effect of the Addition of Ethylene‐propylene Random Copolymers on the Properties of High‐density Polyethylene/Isotactic Polypropylene Blends: Part 1—morphology and Impact Behavior of Molded Samples, *Polym. Eng. Sci.,* 1982, **22**, 536-544.

20 L. D'Orazio, C. Mancarella, E. Martuscelli, G. Cecchin and R. Corrieri, Isotactic Polypropylene/Ethylene-Co-Propylene Blends: Effects of the Copolymer Microstructure and

Content on Rheology, Morphology and Properties of Injection Moulded Samples, *Polymer,* 1999, **40**, 2745-2757.

21 L. D'Orazio and G. Cecchin, Isotactic Polypropylene/Ethylene-Co-Propylene Blends: Effects of Composition on Rheology, Morphology and Properties of Injection Moulded Samples, *Polymer,* 2001, **42**, 2675-2684.

22 Z. Horváth, A. Menyhárd, P. Doshev, M. Gahleitner, D. Friel, J. Varga and B. Pukánszky, Improvement of the Impact Strength of Ethylene‐propylene Random Copolymers by Nucleation, *J Appl Polym Sci,* 2016, **133,** 43823.

23 D. Van der Meer, Structure-Property Relationships in Isotactic Polypropylene, *University of Twente,* (PhD Thesis), 2003.

24 F. Aubin, Flow-Induced Crystallization of Isotactic Polypropylene and Random Polyethylene-Polypropylene Copolymers, *University of Nebraska-Lincoln,* (M.S. Thesis), 2013.

25 K. Kim, M. W. Schulze, A. Arora, R. M. Lewis, M. A. Hillmyer, K. D. Dorfman and F. S. Bates, Thermal Processing of Diblock Copolymer Melts Mimics Metallurgy, *Science,* 2017, **356**, 520-523.

26 J. M. Eagan, J. Xu, R. Di Girolamo, C. M. Thurber, C. W. Macosko, A. M. LaPointe, F. S. Bates and G. W. Coates, Combining Polyethylene and Polypropylene: Enhanced Performance with PE/iPP Multiblock Polymers, *Science,* 2017, **355**, 814-816.

28 C. Choy, W. Luk and F. Chen, Thermal Conductivity of Highly Oriented Polyethylene, *Polymer,* 1978, **19**, 155-162.

29 C. Choy, Y. Wong, G. Yang and T. Kanamoto, Elastic Modulus and Thermal Conductivity of Ultradrawn Polyethylene, *J. Polym. Sci. , Part B: Polym. Phys.,* 1999, **37**, 3359-3367.

30 S. Shen, A. Henry, J. Tong, R. Zheng and G. Chen, Polyethylene Nanofibres with very High Thermal Conductivities, *Nat. Nanotechnol.,* 2010, **5**, 251-255.

31 J. Loomis, H. Ghasemi, X. Huang, N. Thoppey, J. Wang, J. K. Tong, Y. Xu, X. Li, C. Lin and G. Chen, Continuous Fabrication Platform for Highly Aligned Polymer Films, *Technology,* 2014, **2**, 189-199.

32 G. Kim, D. Lee, A. Shanker, L. Shao, M. S. Kwon, D. Gidley, J. Kim and K. P. Pipe, High Thermal Conductivity in Amorphous Polymer Blends by Engineered Interchain Interactions, *Nature materials,* 2015, **14**, 295.

33 T. Ohara, T. Chia Yuan, D. Torii, G. Kikugawa and N. Kosugi, Heat Conduction in Chain Polymer Liquids: Molecular Dynamics Study on the Contributions of Inter-and Intramolecular Energy Transfer, *J. Chem. Phys.,* 2011, **135**, 034507.

34 T. Zhang and T. Luo, Morphology-Influenced Thermal Conductivity of Polyethylene Single Chains and Crystalline Fibers, *J. Appl. Phys.,* 2012, **112**, 094304.

35 T. Zhang and T. Luo, Reversible Thermal Conductivity Regulation Utilizing the Phase Transition of Polyethylene Nanofibers, *ACS Nano,* 2013, **7**, 7592-7600.

36 H. Matsubara, G. Kikugawa, T. Bessho, S. Yamashita and T. Ohara, Molecular Dynamics Study on the Role of Hydroxyl Groups in Heat Conduction in Liquid Alcohols, *Int. J. Heat Mass Transfer,* 2017, **108**, 749-759.

37 R. Ma, D. Huang, T. Zhang and T. Luo, Determining influential descriptors for polymer chain conformation based on empirical force-fields and molecular dynamics simulations, *Chem. Phys. Lett.*, 2018, **704**, 49-54.

38 S. Plimpton, P. Crozier and A. Thompson, LAMMPS-Large-Scale Atomic/Molecular Massively Parallel Simulator, http://Lammps.Sandia.Gov., *Sandia National Laboratories,* 2007.

39 J. W. Ponder and F. M. Richards, An Efficient Newton‐like Method for Molecular Mechanics Energy Minimization of Large Molecules, *J. Comput. Chem.,* 1987, **8**, 1016-1024.

40 J. W. Ponder, TINKER: Software Tools for Molecular Design, *Washington University School of Medicine, Saint Louis, MO,* 2004.

41 W. L. Jorgensen, D. S. Maxwell and J. Tirado-Rives, Development and Testing of the OPLS all-Atom Force Field on Conformational Energetics and Properties of Organic Liquids, *J. Am. Chem. Soc.,* 1996, **118**, 11225-11236.

42 D. Torii, T. Nakano and T. Ohara, Contribution of Inter-and Intramolecular Energy Transfers to Heat Conduction in Liquids, *J. Chem. Phys.,* 2008, **128**, 044504.

43 T. Ohara, T. C. Yuan, D. Torii, G. Kikugawa and N. Kosugi, Heat Conduction in Chain Polymer Liquids: Molecular Dynamics Study on the Contributions of Inter-and Intramolecular Energy Transfer, *J. Chem. Phys.,* 2011, **135**, 034507.

44 G. Kikugawa, T. Ohara, T. Kawaguchi, I. Kinefuchi and Y. Matsumoto, A Molecular Dynamics Study on Heat Conduction Characteristics Inside the Alkanethiolate SAM and Alkane Liquid, *Int. J. Heat Mass Transfer,* 2014, **78**, 630-635.

45 S. Wang, Y. Si, J. Yuan, B. Yang and H. Chen, Tunable Thermal Transport and Mechanical Properties of Graphyne Heterojunctions, *Phys. Chem. Chem. Phys.,* 2016, **18**, 24210-24218.

46 T. Luo and G. Chen, Nanoscale Heat Transfer–from Computation to Experiment, *Phys. Chem. Chem. Phys.,* 2013, **15**, 3389-3412.

47 T. Lezon, Statistical Mechanics of Chain Molecules: An Overview, http://ccbb.pit*t.edu/Faculty/lezon/teaching/smcm. pdf*.

48 D. Torii, T. Nakano and T. Ohara, Contribution of Inter-and Intramolecular Energy Transfers to Heat Conduction in Liquids, *J. Chem. Phys.,* 2008, **128**, 044504.
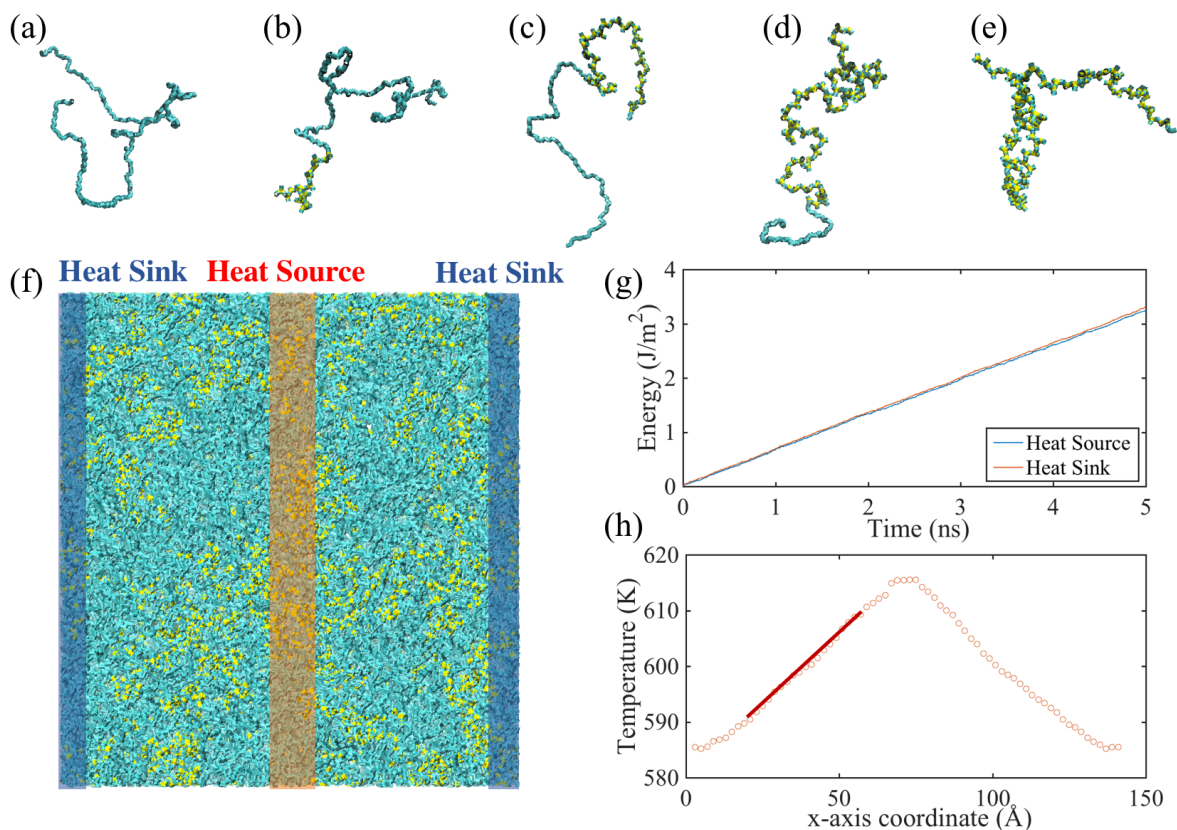
Figure 1. Structures of a single copolymer chain for (a) pure PE with 200 carbons (100 monomers), (b) PE-PP diblock copolymer with 20% PP content, (c) PE-PP diblock copolymer with 50% PP content, (d) PE-PP diblock copolymer with 80% PP content, and (e) pure PP with 300 carbons (100 monomers) on the chain. (f) The simulation domain with 400 block copolymer chains in the amorphous state and the NEMD thermostat setup on the simulation box. (g) The cumulative energy input and output in the thermostated regions from the NEMD simulation. (h) Steady state temperature profile from the NEMD simulation.
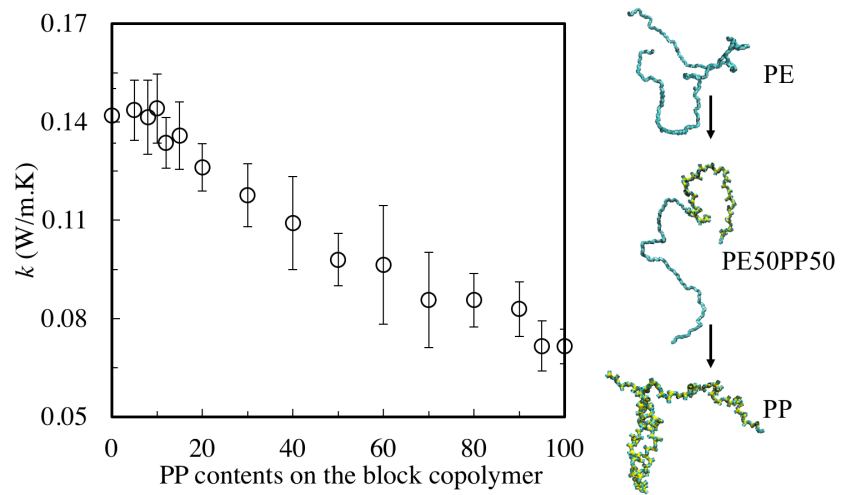
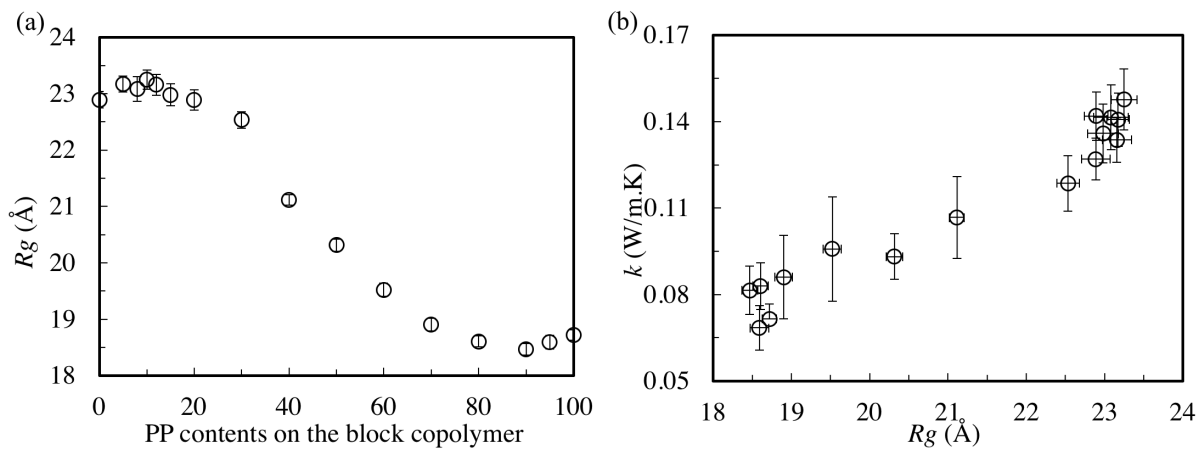**Figure 2**. The relationship between the thermal conductivity the PP block ratio at 600 K.

Figure 3. (a) The R_g of block copolymer as a function of the PP block ratio at 600 K. (b) The relationship of the thermal conductivity and the corresponding R_g.
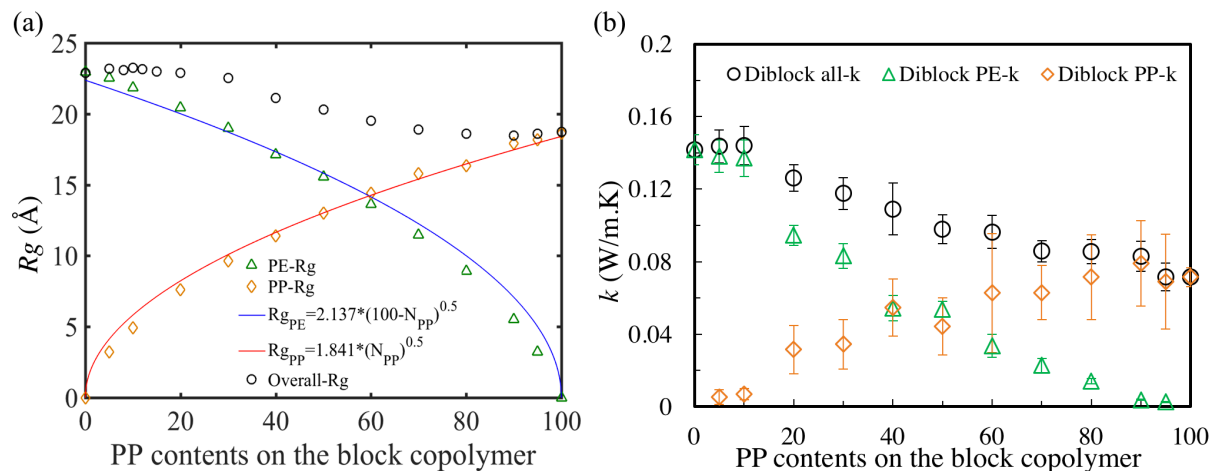
3

Figure 4. (a) The R_g of the PP portion (orange diamond PP-R_g) and the PE portion (green triangle PE-R_g) as a function of the PP block ratio. (b) The thermal conductivity contributions from the PP portion (orange diamond PP-k) and the PE portion (green triangle PE-k) as a function of the PP block ratio.
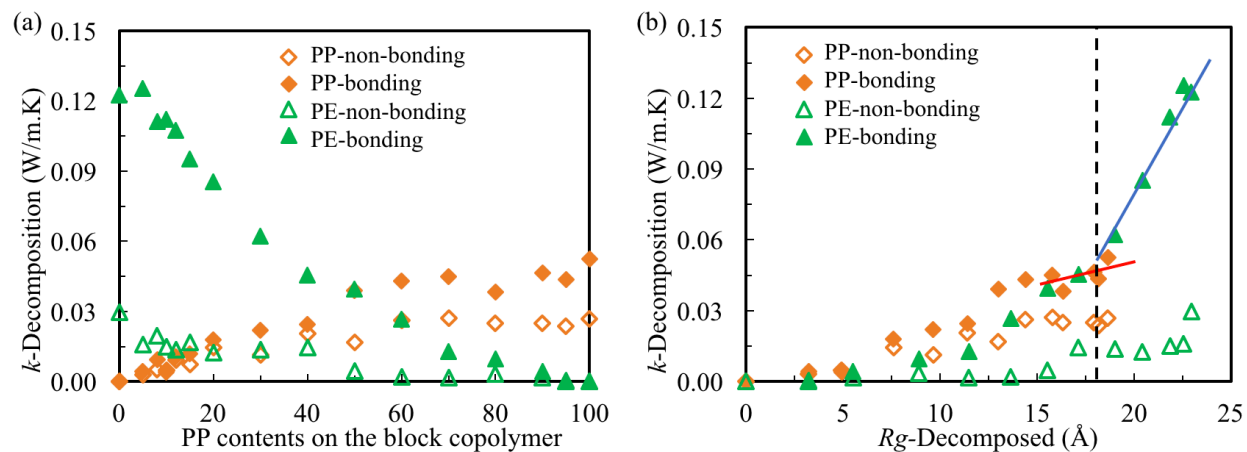
Figure 5. (a) Thermal conductivity contributions from the bonding (closed green triangle) and non-bonding (open green triangle) interactions of the PE portion and the bonding (closed orange diamond) and non-bonding (open orange diamond) interactions of the PP portion. (b) The relationship between the decomposed thermal conductivity and the corresponding R_g of the PE and PP portions.